

magnitudes of hadronic and leptonic contributions to charge renormalization in this model.

ACKNOWLEDGMENTS

The authors are deeply indebted to Professor Abdus Salam and Dr. J. Strathdee for helpful dis-

cussions. One of the authors (PG) acknowledges many useful discussions with Professor G. Mohan and Dr. J. N. Passi. They would also like to thank Professor Abdus Salam, the International Atomic Energy Agency, and UNESCO for hospitality at the International Centre for Theoretical Physics, Trieste.

*On deputation from the Department of Physics, Visva-Bharati University, Santiniketan 731235, West Bengal, India.

¹T. D. Lee and B. Zumino, in *Old and New Problems in Elementary Particles* (Academic, New York, 1968).

²N. M. Kroll, T. D. Lee, and B. Zumino, *Phys. Rev.* 157, 1376 (1967).

³D. Capper, *Phys. Rev. D* 4, 377 (1971).

⁴D. M. Capper and P. Ghose, preceding paper, *Phys. Rev. D* 8, 3588 (1973).

⁵P. R. Auvil and N. G. Deshpande, *Phys. Rev. D* 6, 2213 (1972).

⁶ $C(p^2)$ is related to $\Pi(p^2)$ of Refs. 3 and 4 by $\Pi(p^2) = p^2 C(p^2)$.

⁷For details we refer to Ref. 1 and also to G. C. Wick, in *Selected Topics in Particle Physics*, Proceedings of the International School of Physics "Enrico Fermi," Course XLI (Academic, New York, 1968).

⁸K. Johnson, *Nucl. Phys.* 25, 435 (1961).

Reggeon Structure, s -Channel Unitarity, and the Mandelstam Cut

I. G. Halliday and C. T. Sachrajda

Department of Physics, Imperial College, London SW7 2BZ, England

(Received 20 March 1973)

We study in detail the allowed s -channel intermediate states in the unitarity equations for the Mandelstam and Amati-Fubini-Stanghellini diagrams. The aim is to contrast them with Abarbanel's analysis of the full unitarity equation. On this basis we argue that Abarbanel's ansatz for the general production amplitude is incomplete. The details of our calculation depend strongly on the off-mass-shell behavior of the ladder diagrams which we analyze in some detail. Our analysis is also generalized to present arguments against the inclusive-sum-rule *proof* of the vanishing of the triple-Pomeron vertex at $t = 0$.

I. INTRODUCTION

Recently two opposite conclusions have been reached concerning the sign of the two-Reggeon cut contribution to the total cross section. Abarbanel¹ gave an argument based on a decomposition of the s -channel unitarity equation and claimed a definite positive sign. White,² on the other hand, has given an analysis, using the t -channel unitarity equation continued to complex angular momentum, which gives a definite negative answer.

In this paper we wish to study Abarbanel's decomposition in the context of weak-coupling ϕ^3 perturbation theory. In this context we show that his ansatz for the production amplitudes is incomplete. If the ansatz is incomplete in this simplest of unitary (s and t channels) models, we fail to see how it is justified in the case of the real world. The essential point is that two-Reggeon cuts may

arise in, at least, two ways. First, one may put a Regge pole in T , another in T^* , and convolute them in the classic Amati-Fubini-Stanghellini³ (AFS) manner to obtain the cut using the s -channel unitarity equation as in Fig. 1. However, one may also put a production amplitude in T and a production amplitude convoluted with a Reggeon in T^* such that when the unitarity equation joins the production amplitudes, they give rise to a Regge pole and hence to a cut through the convolution (cf. Fig. 2). This latter method is, we believe, available in any conceivable model of the Pomeron except that the Pomeron is some kind of elementary, structureless, singularity. Because of the nonfactorizability which our analysis of the Mandelstam diagram will clarify, it is difficult to see how s -channel techniques will be able to cope with this complexity.

We realize that many models have been con-

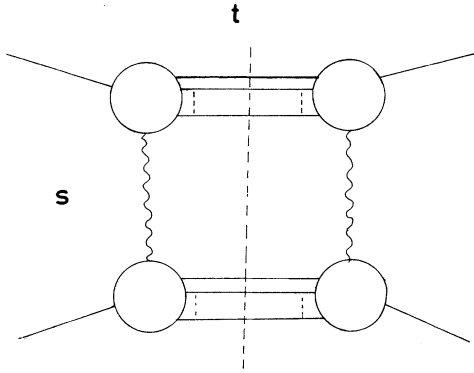


FIG. 1. The AFS cut mechanism. Wiggly lines represent Reggeon exchange.

structured which give rise to negative cuts through absorptive effects.⁴ Since these models do not possess unitary properties in the Reggeon t channels, comparison with White's² analysis is difficult. Also since they always compute effectively the AFS cuts, which probably should cancel, one has doubts about their calculation. We therefore believe that the calculation of the Mandelstam diagram cut using s -channel unitarity is of some interest.

In the course of analyzing the AFS³ diagram and, in particular, the cancellation of the cut in this diagram, we were rather surprised to find that the cancellation depended strongly on the ladder diagrams *not* going to zero rapidly when an external mass $M^2 \rightarrow \infty$ with $s/M^2 \rightarrow \infty$. This result is not in contradiction with the analysis of Rothe or Gribov⁵ of this problem as the crucial behavior for their application of Cauchy's theorem occurs for $s/M^2 \rightarrow 0$.

The plan of the paper is as follows. In Sec. II we describe the behavior of ladder diagrams at high energies s when one or more external masses $M_i^2 \rightarrow \infty$ such that $s/M_i^2 \rightarrow \infty$. The derivation of these results is given in the Appendix. These results are used in Sec. III to show which s -channel intermediate states of the AFS-Feynman diagram cancel the AFS two-particle intermediate state. The

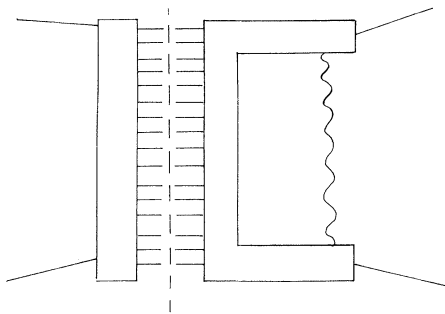


FIG. 2. Another cut mechanism.

importance and general significance of the off-shell behavior is then discussed. In Sec. IV a similar analysis is then carried out for the Mandelstam diagram and the known minus sign derived for these diagrams. In Sec. V we use these results to sharpen our disagreement with Abarbanel's analysis. In Sec. VI we analyze the derivation⁶ of the zero at $t=0$ in the triple-Pomeron vertex using inclusive sum rules due to DeTar and Weis. We show that this proof depends on assumptions which are false in ϕ^3 perturbation theory. Thus, to obtain the result we are forced back to the t -channel proofs.

II. OFF-SHELL BEHAVIOR

In our calculations of the cut contributions we will repeatedly require the asymptotic forms of the ladder diagrams both on and off the mass shell. We shall give the matrix elements of $\hat{S} = \hat{1} + i(2\pi)^4 \hat{T}$ between states

$$|p_1 \cdots p_n\rangle = \prod_1^n a^+(p_i) |0\rangle,$$

where

$$[a^-(p), a^+(q)] = (2\pi)^3 2E(p) \delta^3(p-q).$$

Thus we have positive imaginary parts of two-body amplitudes in order to obtain positive cross sections.

Thus, for the on-shell amplitude of Fig. 3, we have for the uncrossed ladder⁷

$$\begin{aligned} T_m^a \approx & -g^2 \frac{[K(t)(\ln s - i\pi)]^m}{s(m!)} \\ & + B_m(t) \frac{(\ln s - i\pi)^{m-1}}{s} \quad (|s| \rightarrow \infty, t \text{ finite}) \\ & + \cdots, \end{aligned} \quad (2.1)$$

where the two minus signs in the first term are determined by the two criteria that $\text{Im}T \geq 0$ for $s = |s| + i\epsilon$ and $\text{Im}T = 0$ for real $s < 0$. Similarly $B_m(t)$ must be real.

The crossed ladder then gives

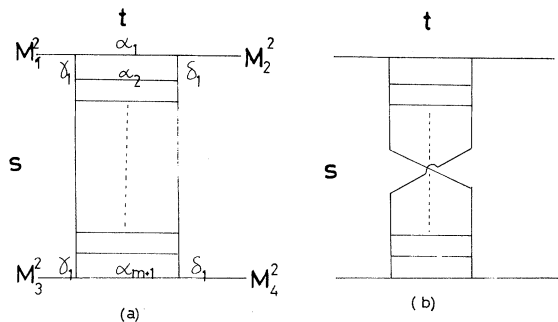


FIG. 3. The crossed and uncrossed ladders.

$$T_m^b(s) = T_m^a(4m^2 - t - s) \approx \frac{g^2 [K(t) \ln s]^m}{s(m!)} + \frac{B_m^1(t) (\ln s)^{m-1}}{s} \quad (2.2)$$

for $s \rightarrow +\infty$ along the real axis with $B_m^1(t)$ real. This real form agrees with the fact that T^b has no right-hand cut in s .

Notice that for $s \rightarrow \infty$ along the positive real axis,

$$T_m = T_m^a + T_m^b \approx \frac{i\pi g^2}{s} \frac{[K(t)]^m}{(m-1)!} (\ln s)^{m-1}. \quad (2.3)$$

Thus the signed ladders, i.e., the sum of crossed and uncrossed ladders lose a power of $\ln s$ compared with the uncrossed ladders. This is absolutely crucial for our calculations.

The function $K(t)$, which is positive definite for $t < 0$, is given by

$$K(t) = \frac{-g^2}{16\pi^2} \int_0^1 \frac{d\beta_1 d\beta_2 \delta(\beta_1 + \beta_2 - 1)}{(\beta_1 \beta_2 t - m^2)} = \frac{g^2}{16\pi^3} \int \frac{d^2\kappa}{(\kappa^2 + m^2)[(\kappa + q)^2 + m^2]}, \quad (2.4)$$

where κ, q are Euclidean and $t = -q^2$.

If only one mass squared $M_i^2 \rightarrow \infty$ the above formula becomes, for $s, M_i^2 < 0$, and s/M_i^2 large,

$$T_m^a \approx -\frac{g^2}{m!s} [K(t) \ln(s/M_i^2)]^m. \quad (2.5)$$

If both M_1^2 and $M_2^2 \rightarrow \infty$, then for $s < 0$ and s/M_i^2 large,

$$T_m^a \approx -\frac{g^2}{m!s} [K(t) \ln(s/N^2)]^m, \quad (2.6)$$

where $N^2 = \max(M_1^2, M_2^2)$.

If one mass at the top M_α^2 ($\alpha = 1$ or 2) and one at the bottom M_β^2 ($\beta = 3$ or 4) tend to minus infinity, then

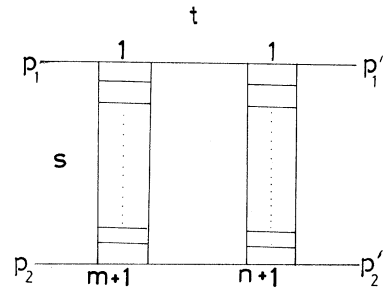


FIG. 4. The AFS Feynman diagram.

$$T_m^a \approx -\frac{g^2}{m!s} \left[K(t) \ln \frac{-s}{M_\alpha^2 M_\beta^2} \right]^m, \quad (2.7)$$

provided $s/M_\alpha^2 M_\beta^2$ is large.

The case (2.7) for $M_1^2 \sim M_2^2 \sim s$ has previously been studied by Altarelli and Rubinstein.⁸ The correction terms to (2.5), (2.6), and (2.7) are easily obtained by altering the arguments of the logarithms in (2.1) and (2.2) to agree with the leading terms.

Notice that although we let $M_i^2 \rightarrow \infty$, we always insist on s/M_i^2 being large. This means that in the region we are considering, these amplitudes never become small.

We would like to stress that the analysis of any given diagram changes dramatically when we turn to the limit $s/M_i^2 \rightarrow 0$ and the result (2.5), for example, is certainly *not* applicable.

III. THE AFS CANCELLATION

We wish to show that the Feynman diagram of Fig. 4 does not possess the cut which is present in the discontinuity of the amplitude across its two-particle cut in the s channel shown in Fig. 5(a). To do this we show that the leading behavior of the unitarity cut of Fig. 5(a) is exactly canceled by the two cuts of Fig. 5(b) and Fig. 5(c).

This result is, of course, known from other

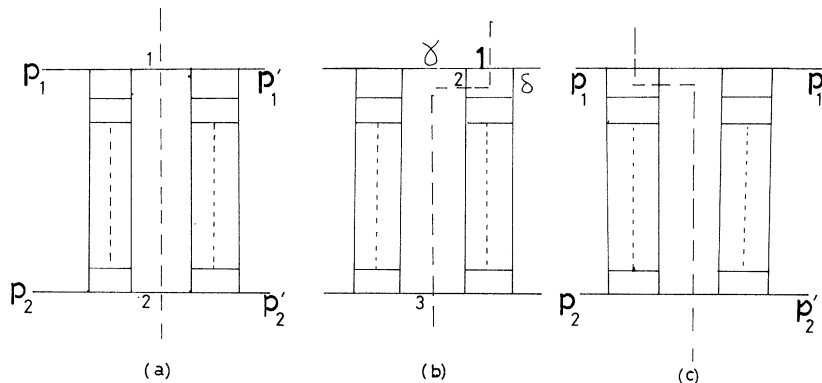


FIG. 5. Three canceling s -channel intermediate states.

techniques. Thus Polkinghorne⁹ computed the full Feynman diagram and showed it had no cut. Mandelstam⁹ showed the same result essentially using *t*-channel unitarity. Rothe and Gribov⁵ also calculated the Feynman diagram directly using an apparently simpler technique. Nicoletopoulos and Prevost⁹ have carried out an analysis of these Feynman diagrams using Cauchy's theorem, which is similar in spirit to our analysis. However it is very hard to unravel the unitarity equation from their analysis, and indeed we disagree with their statements about the AFS cancellation.

We carry out the calculation in the *s* channel for

$$2 \operatorname{Im} T = \sum_{r=2}^{\infty} \frac{1}{(2\pi)^{3r-4} r!} \int \prod_{i=1}^r [d^4 q_i \delta^+(q_i^2 - m^2)] T_{2r} T_{2r}^* \delta^4 \left(p_1 + p_2 - \sum_1^r q_i \right). \quad (3.1)$$

The $r!$ in (3.1) comes from the identity of the r particles in the intermediate state. This will always be canceled in our calculations by the fact that there are also always $r!$ Feynman diagrams corresponding to the different ways of labeling the final-state particles. Thus we drop it and only draw one of the $r!$ diagrams.

In general we also do not calculate $\operatorname{Im} T$ but only the various terms corresponding to the discontinuities across the individual normal thresholds. Thus we label the left-hand sides by $(1/i)\Delta_a T$.

We shall always label the on-shell intermediate-state particles by $1, \dots, r$. For the contribution of Fig. 5(a) we have

$$\begin{aligned} \frac{1}{i} \Delta_a T = & \frac{1}{(2\pi)^2} \int d^4 q_1 d^4 q_2 \delta^+(q_1^2 - m^2) \delta^+(q_2^2 - m^2) \\ & \times \delta^4(q_1 + q_2 - p_1 - p_2) T_m^a T_n^{a*}, \end{aligned} \quad (3.2)$$

with T_m^a given by Eq. (2.1) since the external particles of the ladder are all on-shell.

We shall use Sudakov¹⁰ variables throughout. Thus we write

$$\begin{aligned} q_i = & \alpha_i [p_1 - (m^2/s)p_2] + \beta_i [p_2 - (m^2/s)p_1] + \kappa_i, \\ \kappa \cdot p_i = & 0 \end{aligned} \quad (3.3)$$

and, as usual,

$$\begin{aligned} d^4 q_i \delta^+(q_i^2 - m^2) = & \frac{1}{2} |s| d\alpha_i d\beta_i d^2 \kappa_i \delta(\alpha_i \beta_i s - \mu_i^2), \\ \mu_i^2 = & m^2 - \kappa_i^2 \end{aligned} \quad (3.4)$$

where κ_i is purely spacelike. Finally

$$\begin{aligned} \delta^4(p_1 + p_2 - \sum q_i) = & \delta(\sum \alpha_i - 1) \delta(\sum \beta_i - 1) \\ & \times \delta(\sum \kappa_i) \frac{2}{|s|}. \end{aligned} \quad (3.5)$$

two reasons. First, we wish to check our technique, and, second, we wish to stress the identical nature of this calculation and the inclusive-sum-rule calculations of Sec. VI.

To calculate the imaginary part for $s > 0$ of the diagram of Fig. 4, we have two options open. Either we can use the unitarity equation $\operatorname{Im} T = \frac{1}{2} T T^\dagger$ or we can use the Cutkosky prescription. This latter technique involving multiple cuts in the *s* channel is necessarily more complicated so we use the unitarity equation.

The contribution from Fig. 5(a) is calculated using the unitarity equation:

Thus (3.2) becomes

$$\begin{aligned} \frac{1}{i} \Delta_a T = & \frac{2}{(2\pi)^2} \int \frac{d\alpha_1}{2\alpha_1} \frac{d\beta_2}{2\beta_2} \delta(\alpha_1 + \alpha_2 - 1) \\ & \times \delta(\beta_1 + \beta_2 - 1) T T^* d^2 \kappa_1 d^2 \kappa_2 \\ & \times \delta(\kappa_1 + \kappa_2). \end{aligned} \quad (3.6)$$

Now the momentum transfer down the left ladder is given by

$$t_L \simeq -(1 - \alpha_1)\beta_1 s + \kappa_1^2.$$

For this to remain finite as $s \rightarrow \infty$ implies $\beta_1 \sim 1/s$ and therefore $\alpha_1 \sim \text{constant}$. Thus $\beta_2 \sim 1$, therefore $\alpha_2 \sim 1/s$, and so $\alpha_1 \sim 1$. Therefore

$$\begin{aligned} \frac{1}{i} \Delta_a T = & \frac{1}{8\pi^2 s} \int T T^* d^2 \kappa_1 \\ \simeq & \frac{1}{8\pi^2} \frac{g^4}{m! n! s^3} \int K(t_L)^m K(t_R)^n (\ln s)^{m+n} d^2 \kappa, \end{aligned} \quad (3.7)$$

where $t_2 = -|\kappa_1|^2$, and if p'_1 has Sudakov parameters $(1, 0, p_\perp)$ then $t_R = -|(p_\perp - \kappa)|^2$ and $t = -|p_\perp|^2$.

Now turn to Fig. 5(b). We have a three-particle intermediate state. The two T matrices for the left and right portions of the diagram are

$$\begin{aligned} T^L = & T_m^a \frac{i(-ig)}{(k_\gamma^2 - m^2)}, \\ T^R = & T_{n-1}^a \frac{i(-ig)}{(k_\delta^2 - m^2)}, \end{aligned} \quad (3.8)$$

where the ladders in T^a have external masses off shell and the right-hand ladder has lost a rung:

$$\frac{1}{i} \Delta_b T \simeq \frac{2}{(2\pi)^5 |s|} \int \frac{d\alpha_1}{2\alpha_1} \frac{d\alpha_2}{2\alpha_2} \frac{d\beta_3}{2\beta_3} \delta(\alpha_1 + \alpha_2 + \alpha_3 - 1) \times d^2\kappa_1 d^2\kappa_2 \delta(\beta_1 + \beta_2 + \beta_3 - 1) \times T^L T^R^* \quad (3.9)$$

In order that the momentum transfers down the ladders remain finite, it is clear that $\alpha_3 \rightarrow 0$, $\beta_1 + \beta_2 \rightarrow 0$. Therefore, using $\beta_3 \sim 1$,

$$\frac{1}{i} \Delta_b T \simeq \frac{1}{s(2\pi)^5 4} \int_0^1 \frac{d\alpha_1}{\alpha_1} \frac{d\alpha_2}{\alpha_2} \delta(\alpha_1 + \alpha_2 - 1) d^2\kappa_1 d^2\kappa_2 \times T_m^a T_{n-1}^a \frac{1}{(k_\gamma^2 - m^2)(k_\delta^2 - m^2)} \quad (3.10)$$

The amplitudes T^a are given by

$$T_m^a = \frac{-g^2 K^m [\ln(s/M_\gamma^2)]^m}{s(m!)} \quad (3.11)$$

$$T_{n-1}^a \simeq -g^2 \frac{K^{n-1} (\ln s')^{n-1}}{s'(n-1)!}$$

where

$$s' \simeq (\alpha_2 + \alpha_3)(\beta_2 + \beta_3)s \simeq \alpha_2 s$$

$$M_\gamma^2 \simeq (\alpha_1 + \alpha_2) \left(\frac{\mu_1^2}{\alpha_1} + \frac{\mu_2^2}{\alpha_2} \right) + (\kappa_1 + \kappa_2)^2 = k_\gamma^2$$

As it stands, the integrand of (3.10) contains one power of $\ln s$ less than (3.7). Thus, for any significant cancellation to occur, we must regain the power of $\ln s$. This comes from a nonuniformity in the α integrals. Consider the region where $\alpha_1 \gg \alpha_2$. Then (3.10) becomes

$$\frac{1}{i} \Delta_b T \simeq \frac{1}{s^2 (2\pi)^5 4} \int \frac{d\alpha_2}{\alpha_2} d^2\kappa_1 d^2\kappa_2 \frac{g^6 K^m(t_L) K^{n-1}(t_R)}{m!(n-1)!} \times \frac{[\ln(\alpha_2 s)]^{m+n-1}}{(\mu_2^2/\alpha_2)(-\mu_\delta^2)(\alpha_2 s)} \quad (3.12)$$

since $M_\gamma^2 \simeq \mu_2^2/\alpha_2 \rightarrow \infty$, and

$$k_\delta^2 \simeq -(1 - \alpha_1)\beta_1 s + (\kappa_1 - p_1)^2 \simeq (\kappa_1 - p_1)^2$$

Notice in particular the fact that $M_\gamma^2 \rightarrow \infty$ so that we must use (2.5) for T^L . The limits on the α_2 integral are set by the two criteria $s' \geq M_0^2$ and $M_\gamma^2 \geq M_0^2$, where M_0^2 is a large positive mass squared which sets the asymptotic scale of our theory. Thus we integrate α_2 from M_0^2/s to μ_2^2/M_0^2 . This integral can be performed, and we find the leading term

$$\frac{-g^6}{(2\pi)^5 4 s^3} \int \frac{d^2\kappa_1 d^2\kappa_2 (\ln s)^{m+n}}{\mu_2^2 \mu_\delta^2 m!(n-1)!(m+n)} K(t_L)^m K(t_R)^{n-1} \quad (3.13)$$

The combination $1/\mu_2^2 \mu_\delta^2$ is, of course, just correct to produce an extra $K(t_R)$. Therefore

$$\frac{1}{i} \Delta_b T \simeq -\frac{g^4}{s^3 \pi^2 8} \frac{(\ln s)^{m+n}}{(m+n)m!(n-1)!} \int d^2\kappa K(t_L)^m K(t_R)^n \quad (3.14)$$

where $\kappa = \kappa_1 + \kappa_2$ and $t_2 = -|\kappa|^2$, $t_R = -|(p_1 - \kappa)|^2$. The diagram of Fig. 5(c) clearly gives a symmetric answer, and if we add them we obtain

$$\frac{1}{i} \Delta_{b+c} T \simeq \frac{-g^4 (\ln s)^{m+n}}{8\pi^2 s^3 m! n!} \int d^2\kappa K^m K^n \quad (3.15)$$

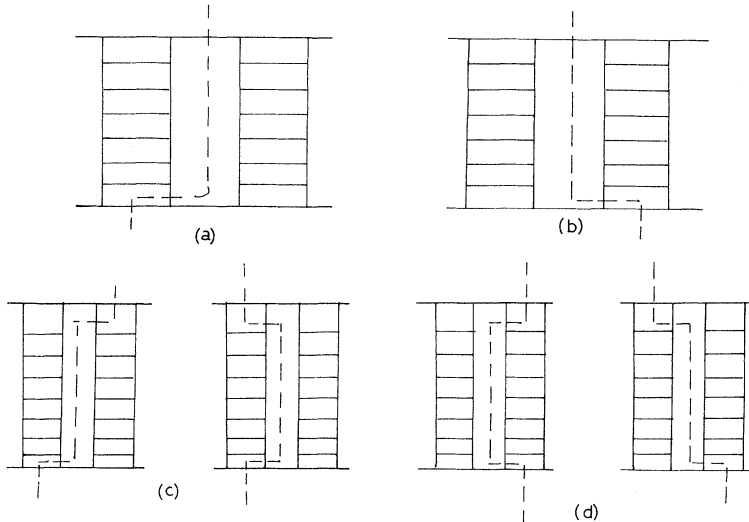


FIG. 6. The other intermediate states at the bottom of the diagram.

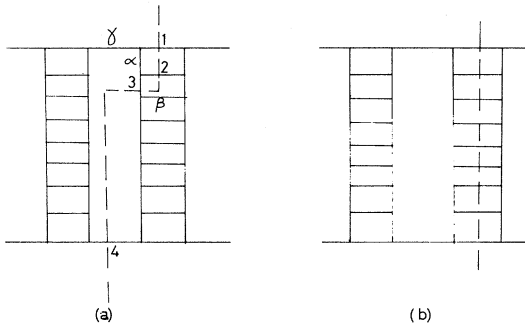


FIG. 7. Two nonleading intermediate states.

It is a straightforward matter to check that no other parts of the allowed α_1, α_2 region give rise to this enhanced $\ln s$ behavior. Notice that the use of the off-shell behavior for T^L was crucial, otherwise we would not have obtained cancellation. It is also clear that if the large M^2 limit for $s/M^2 \rightarrow \infty$ had been zero, then we would not have increased the power of $\ln s$ in performing the α_2 integral.

The further cuts of Fig. 6(a) and Fig. 6(b) each give an identical contribution to (3.15), which are of course canceled against the cuts of Fig. 6(c) and Fig. 6(d). Notice that this implies that the cancellation takes place at either end, regardless of what is happening at the other end. This is presumably the statement that, for cuts to occur, we need fixed poles at both ends.

Notice that since $\alpha_1 + \alpha_2 \leq 1$ we have $M_\gamma^2 \leq s$ and never greater. The Cauchy theorem proof of this cancellation⁵ for given fixed large s relies on effectively moving a contour in the M_γ^2 plane off to infinity. Thus, necessarily, it must consider $|M_\gamma^2| \gg s$ for the contour at infinity and the amplitudes are zero in that region.

There are of course other cuts of the AFS diagram. First, one may chop two rungs off the ladder in Fig. 7(a). However we then lose two powers of $\ln s$ since the right-hand ladder has lost two

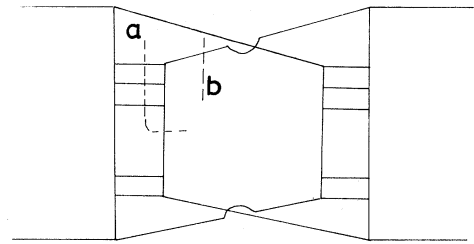


FIG. 9. Two mass cuts.

rungs. Since 1, 2, and 3 are on-shell and therefore timelike, if we let the energy $s_{2\beta}$ get large as in (3.12), then both the α, γ propagators tend to zero. This eliminates the possibility of building up the two powers of $\ln s$. Second, one may cut the ladder as in Fig. 7(b). This is automatically down one power in $\ln s$ since the leading term in (2.1) is real and the right-hand side of Fig. 7(b) contains the imaginary part of T^a . In fact, one can easily show in general by the arguments of Ref. 4 that Fig. 7(b) gives rise to no cut.

IV. THE MANDELSTAM CUT

We wish to show which s -channel cuts of the diagrams of Fig. 8 give rise to the dominant asymptotic behavior and in particular how the minus sign arises. We stress that the minus sign only arises when we consider *signed* amplitudes. In the language of Feynman diagrams, crossed and uncrossed ladders must be added. Indeed we shall show that the simple diagram of Fig. 8(a) with only planar ladders is positive definite at large s .

There are, of course, rather a large number of allowed intermediate states in the s channel which we must study. To simplify things initially we consider only Fig. 8(a) and check the result obtained by Cicuta and Sugar.¹¹ Let us try to systematize these intermediate states. Clearly any intermediate state which cuts one of the lines 1-8 is naturally associated with cuts in that variable of

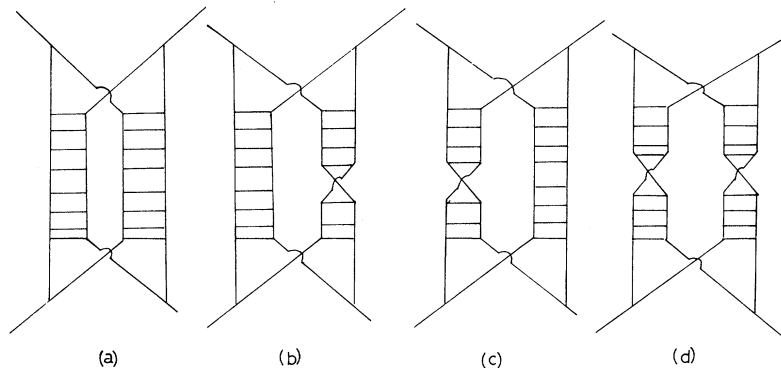


FIG. 8. The signed Mandelstam diagrams.

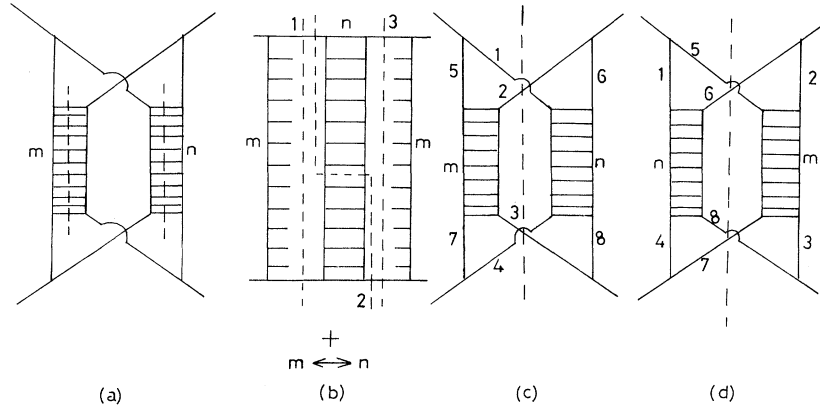


FIG. 10. Counting the Mandelstam cuts.

the ladder. Thus we think of the cuts a, b of Fig. 9 simultaneously. Then we write all possible cuts of Fig. 8(a) in Fig. 10. These may be systematized by considering diagrams where the ladders are and are not cut in the s channel as in Figs. 10(a), 10(b), and 10(c). We would stress that for crossed ladders the appropriate diagrams of Figs. 10(a) and 10(b) are missing.

We would now like to go through the calculations of the various contributions. First, let us calculate the cut of Fig. 11. We find

$$\frac{1}{i}\Delta T = \frac{1}{(2\pi)^8} \int \frac{d^3 q_1}{2E_1} \frac{d^3 q_2}{2E_2} \frac{d^3 q_3}{2E_3} \frac{d^3 q_4}{2E_4} \times \delta^4\left(\sum_1^4 q_i - p_1 - p_2\right) T^L T^R, \quad (4.1)$$

$$T^L = \frac{g}{k_\gamma^2 - m^2} \frac{g}{k_\mu^2 - m^2} T_m^a, \quad (4.2)$$

$$T^R = \frac{g}{k_\delta^2 - m^2} \frac{g}{k_\nu^2 - m^2} T_n^a.$$

To obtain large subenergies in the ladders we must have $\alpha_2 \gg \alpha_3$ and $\alpha_1 \gg \alpha_4$. For finite momentum transfers down the ladders, $\alpha_1 + \alpha_2 \gg \alpha_3 + \alpha_4$.

Thus we obtain

$$\begin{aligned} \frac{1}{i}\Delta T \approx & \frac{1}{2^3 s (2\pi)^8} \int \frac{d\alpha_1}{\alpha_1} \frac{d\alpha_2}{\alpha_2} \delta(\alpha_1 + \alpha_2 - 1) \frac{d\beta_3 d\beta_4}{\beta_3 \beta_4} \\ & \times \delta(\beta_3 + \beta_4 - 1) \prod_1^4 d^2 \kappa_i \\ & \times \delta\left(\sum \kappa_i - 1\right) T^L T^R. \end{aligned} \quad (4.3)$$

As in AFS case, the only place that the integral can enhance the logarithm is at the end points. Assume $\alpha_1 \gg \alpha_2, \beta_3 \gg \beta_4$:

$$\begin{aligned} s_L &= (q_2 + q_3)^2 \approx \alpha_2 \beta_3 s \approx \alpha_2 s, \\ s_R &= (q_1 + q_4)^2 \approx \beta_4 s, \\ k_\gamma^2 &= -(1 - \alpha_1)\beta_1 s + \kappa_1^2 \approx \kappa_1^2, \\ k_\delta^2 &= -(1 - \alpha_2)\beta_2 s = -\mu_2^2/\alpha_2 \rightarrow \infty, \\ k_\nu^2 &= -(1 - \beta_3)\alpha_3 s + \kappa_3^2 \approx \kappa_3^2, \\ k_\mu^2 &= -(1 - \beta_4)\alpha_4 s \approx -\mu_4^2/\beta_4 \rightarrow \infty, \end{aligned} \quad (4.4)$$

Thus this contribution gives

$$\begin{aligned} \frac{1}{i}\Delta' T \approx & \frac{g^8}{2^3 s (2\pi)^8} \int \prod_1^4 d^2 \kappa_i \delta\left(\sum \kappa_i\right) \int \frac{d\alpha_2}{\alpha_2} \frac{d\beta_4}{\beta_4} \frac{[K(t_L) \ln(s_L/k_\mu^2)]^m}{m! s_L} \frac{[K(t_R) \ln(s_R/k_\delta^2)]^n}{n! s_R} \frac{1}{P_\gamma P_\delta P_\mu P_\nu} \\ \approx & \frac{g^8}{8 s (2\pi)^8} \int \prod d^2 \kappa_i \delta\left(\sum \kappa_i\right) \int \frac{d\alpha_2}{\alpha_2} \int \frac{d\beta_4}{\beta_4} \frac{1}{(-\mu_\gamma^2)(-\mu_\nu^2)} \frac{1}{(\mu_2^2/\alpha_2)(\mu_4^2/\beta_4)} \frac{[K(t_L) \ln(\alpha_2 \beta_4 s)]^m}{\alpha_2 s m!} \frac{[K(t_R) \ln(\alpha_2 \beta_4 s)]^n}{\beta_4 s n!}. \end{aligned} \quad (4.5)$$

We now integrate this, insisting that $\alpha_2 \gg \alpha_4$:

$$\frac{1}{i}\Delta' T \approx \frac{g^4}{8\pi^2 s^3} \int \frac{d^2 \kappa [K(t_L)]^{m+1} [K(t_R)]^{n+1}}{m! n! (m+n+1)(m+n+2)} \times (\ln s)^{m+n+2}, \quad (4.6)$$

where $t_L = -|\kappa^2|$, $t_R = -|\kappa - p_1|^2$, and $t = -|p_1|^2$.

Notice that again the μ 's just arrange themselves into the forms required to write them as $K(t_R)$ and $K(t_L)$. We get three further terms from picking the other orderings of (α_1, α_2) and (β_3, β_4) . We would like to stress at this point that these terms are the dominant contribution to the uncrossed ladder Mandelstam diagram. This result agrees

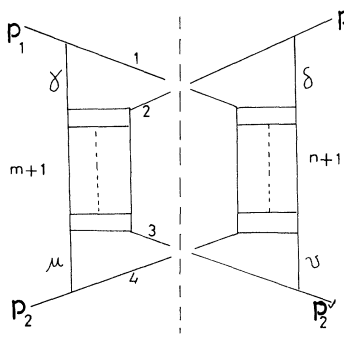


FIG. 11. The unsigned dominant cut.

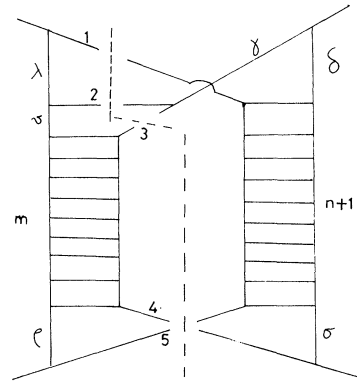


FIG. 12. A nonleading cut.

with the result of Cicuta and Sugar.¹¹

We must obviously, in the light of the AFS cancellation, also calculate the cut shown for example in Fig. 12:

$$\frac{1}{i} \Delta'' T \simeq \frac{1}{(2\pi)^{11} s (2^4)^4} \int \frac{d\alpha_1}{\alpha_1} \frac{d\alpha_2}{\alpha_2} \frac{d\alpha_3}{\alpha_3} \frac{d\beta_4}{\beta_4} \frac{d\beta_5}{\beta_5} \times \delta(\alpha_1 + \alpha_2 + \alpha_3 - 1) \times \delta(\beta_4 + \beta_5 - 1) T_L T_R^* \quad (4.7)$$

$$T_L = \frac{g^3}{(k_\lambda^2 - m^2)(k_\nu^2 - m^2)} T_{m-1}^a \frac{1}{(k_\rho^2 - m^2)},$$

$$T_R = \frac{g^3 T_n^a}{(k_\gamma^2 - m^2)(k_\delta^2 - m^2)(k_\sigma^2 - m^2)}.$$

In order for the AFS trick to work, we need to integrate over the region $\alpha_2 \gg \alpha_3$. Then:

$$k_\gamma^2 - m^2 \simeq (\alpha_2/\alpha_3) \mu_3^2,$$

$$k_\sigma^2 - m^2 \simeq -(1 - \alpha_2)(\beta_3)S + (\kappa_2 + \kappa_3 - p_1)^2,$$

$$k_\lambda^2 - m^2 \simeq -(1 - \alpha_1)\beta_1 s + \kappa_1^2 - m^2,$$

$$k_\nu^2 - m^2 \simeq -(1 - \alpha_1 - \alpha_2)(\beta_1 + \beta_2)S + (\kappa_1 + \kappa_2).$$

(4.8)

The two alternatives now are $\alpha_1 \gg \alpha_2$ or $\alpha_2 \gg \alpha_1$. The first gives:

$$\frac{1}{i} \Delta T = \frac{1}{(2\pi)^6} \int d^4 q_1 d^4 q_2 \delta^+(q_1^2 - m^2) \delta^+(q_2^2 - m^2) d^4 k_a d^4 k_b \delta^4(q_1 + q_2 + k_a + k_b - p_1 - p_2) \times \left\{ \frac{1}{(2\pi)^{3m-1}} \int \left[\prod_{j=1}^{m+1} d^4 k_j \delta^+(k_j^2 - m^2) \right] \delta^4(k_a + k_b - \sum_1^{m+1} k_j) \right\} T_L T_R^* \quad (4.11)$$

where

$$T_L = \frac{g}{(k_\gamma^2 - m^2)(k_\rho^2 - m^2)} \tilde{T}(m),$$

$$T_R = T(m) \left\{ \frac{-1}{(2\pi)^4 (k_a^2 - m^2)(k_b^2 - m^2)} \right\} \left\{ \frac{g^2}{(k_\delta^2 - m^2)(k_\sigma^2 - m^2)} \right\} i T_n^a \quad (4.12)$$

where $\tilde{T}(m)$ is the *T* matrix for the diagram of Fig. 14. In (4.11) we have separated the phase space so

$$\left. \begin{aligned} k_\gamma^2 - m^2 &\simeq \left(\frac{\alpha_2}{\alpha_3} \right) \mu_3^2, \\ k_\delta^2 - m^2 &\simeq -\frac{\mu_3^2}{\alpha_3}, \\ k_\lambda^2 - m^2 &\simeq -\mu_\lambda^2, \\ k_\nu^2 - m^2 &\simeq -\mu_\nu^2, \end{aligned} \right\} \begin{aligned} S_L &\simeq \alpha_3 \beta_4 s, \\ S_R &\simeq \beta_5 s. \end{aligned} \quad (4.9)$$

The α integrals then have the form

$$\int \frac{d\alpha_2 d\alpha_3}{\alpha_2^2} \frac{[\ln(\alpha_3 \beta_4 s)]^{m-1} [\ln(\alpha_3 \beta_5 s)]^n}{(m-1)! \beta_4 s \beta_5 s} \quad (4.10)$$

This clearly does not pick up the requisite 2 powers of lns to compare with the leading term (4.6). One can check the other orderings. This same deboosting occurs in all the external mass cuts in the Mandelstam diagram as is easily, if tediously, checked.

We now turn to the intermediate state of Fig. 13(a) which will ultimately provide us with our negative two-Reggeon cuts. In the uncrossed ladder case they are always at least one power of lns down on (4.6). Let us discuss this in some detail. The first thing to notice is that the lines *a, b* are not on-shell and the Sudakov parameters are integrated from $-\infty$ to $+\infty$ rather than 0 to 1. Thus we consider

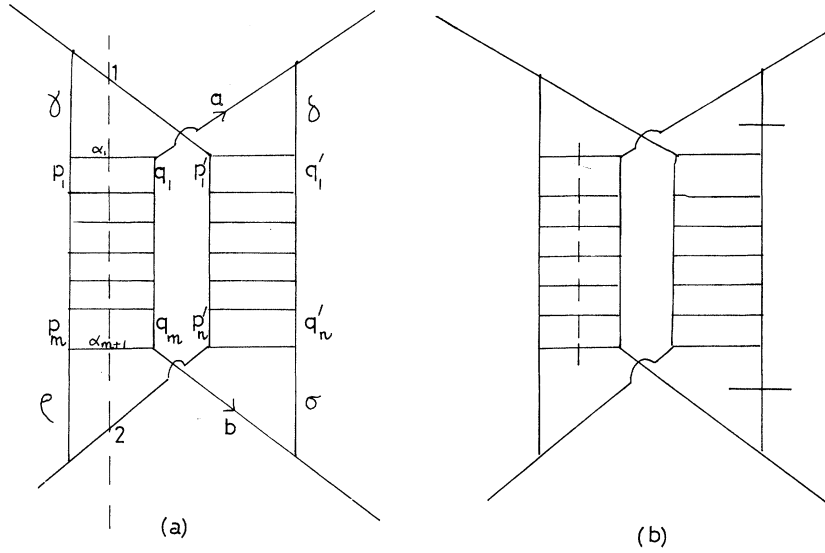


FIG. 13. The Reggeon cuts.

that we obtain from the k_j integrations simply the right-hand side of the unitarity equation for the ladders evaluated with $s = (k_a + k_b)^2$. Thus, finally, we obtain

$$\begin{aligned} \frac{1}{i} \Delta T &= \frac{i g^4}{(2\pi)^{10}} \int \frac{d^3 q_1}{2E_1} \frac{d^3 q_2}{2E_2} \frac{1}{(k_\gamma^2 - m^2)(k_\rho^2 - m^2)} \frac{d^4 k_a}{(k_a^2 - m^2)} \frac{d^4 k_b}{(k_b^2 - m^2)} \delta^4(q_1 + q_2 + k_a + k_b - p_1 - p_2) 2 \text{Im} T_m^a(T_n^a)^* \\ &\simeq \frac{i g^4}{(2\pi)^{10} S} \int \frac{d\alpha_1}{\alpha_1} \frac{d\beta_2}{\beta_2} \frac{\delta(\alpha_1 + \alpha_a - 1) \delta(\beta_2 + \beta_b - 1)}{(k_\gamma^2 - m^2)(k_\rho^2 - m^2)(k_a^2 - m^2)(k_b^2 - m^2)} \frac{1}{2} s d\alpha_a d\beta_a d\alpha_b d\beta_b [\delta(\sum \kappa) \prod d^2 \kappa_i] \text{Im} T_m^a(T_n^a)^*. \end{aligned} \quad (4.13)$$

We have assumed in the above equation that the energies across the ladders must remain large, therefore $\alpha_a \gg \alpha_b$ and $\beta_2 \gg \beta_1$. The subenergies are then given by

$$\begin{aligned} s_L &= (k_a + k_b)^2 \simeq \alpha_a \beta_b s, \\ s_R &= (q_1 + q_2)^2 \simeq \alpha_1 \mu_2^2 / \alpha_2. \end{aligned} \quad (4.14)$$

Now consider the integration in the β_a plane. The singularities in β_a only occur at

$$(a) \quad \alpha_a \beta_a s = m^2 - \kappa_a^2, 4m^2 - \kappa_a^2, \text{ etc.}, \quad (4.15)$$

corresponding to the pole in the a propagator and the mass cuts of the ladder.

$$(b) \quad k_\delta^2 = -(1 - \alpha_a) \beta_a s + \kappa_a^2 = m^2, 4m^2, \text{ etc.},$$

corresponding to the poles in the δ propagator and the appropriate mass cuts of the ladder. In order that these cuts lie on opposite sides of the β_a cut, we must have $0 \leq \alpha_a \leq 1$. The β_a integration is now performed by pulling the contour into the upper half-plane (these poles are in T^*) when we pick up the poles and cuts of (4.15). This pole, with the corresponding pole from the α_b integration, gives us, finally,

$$\begin{aligned} \frac{1}{i} \Delta T &\simeq \frac{-i g^4}{(2\pi)^8} \int \frac{d^3 q_1}{2E_1} \frac{d^3 k_a}{2E_a} \frac{d^3 k_b}{2E_b} \frac{d^3 q_2}{2E_2} \delta(q_1 + q_2 + k_a + k_b - p_1 - p_2) \\ &\quad \times \frac{1}{(k_\gamma^2 - m^2)(k_\rho^2 - m^2)(k_\sigma^2 - m^2)(k_\delta^2 - m^2)} (2 \text{Im} T_m^a)(T_n^a)^*. \end{aligned} \quad (4.16)$$

This is now identical to (4.1), except that we have a $(-i)$ and $T_m^a - 2 \text{Im} T_m^a$. Thus we obtain one power less than the leading term again. Since this term is purely imaginary to leading order, it is of

course canceled to leading order by the cut shown in Fig. 13(b), where the uncut ladder is now in T rather than T^* .

The terms in the contour integral involving the

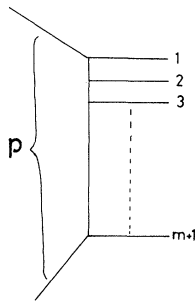


FIG. 14. A Feynman diagram.

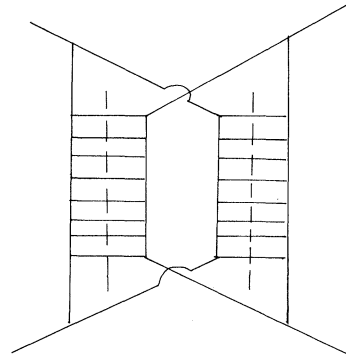


FIG. 16. The two-Reggeon cut.

mass cuts give terms of lower order. This is the same result as that contained in (4.10), so we shall not go through the proof.

The cut through both ladders may be handled in an identical manner and turns out to be two powers of lns down on the leading term.

Now what happens when we turn to the sum of crossed and uncrossed ladders? The leading contributions now have a quite different structure. Thus we must use (2.3) for the amplitude which is purely imaginary now in leading power of lns. This means that unlike the planar case when we cut a ladder in the *s* channel, we do not lose a power of lns as in (4.16). On the other hand, when we add crossed and uncrossed ladders we obtain $i \text{Im} T_m^a$. Moreover in (4.16) to leading order $(T_n^a)^* \rightarrow (T_n^a + T_n^b)^*$, which is purely imaginary so that (4.16) gives a real, negative contribution to the cut, no longer canceled by reality arguments.

Thus the two cuts of Fig. 11(c) give rise to a contribution:

$$\frac{1}{i} \Delta_1 T \approx \frac{g^4}{8s^3(m-1)!(n-1)!} \frac{(+2)}{(m+n)(m+n-1)} \times (\ln s)^{m+n} \int [K(t_L)]^m [K(t_R)]^n \times [K(t_L) + K(t_R)]^2. \quad (4.17)$$

The four cuts of Fig. 15, when the uncut ladders are replaced by the sum of crossed and uncrossed ladders, gives $-(4/i)\Delta_1 T$. Finally the cut down both ladders shown in Fig. 16 may also be easily computed and gives $+(2/i)\Delta_1 T$. We have only one unitary integral unlike Fig. 15, but the amplitude is four times as big as it involves $(2i \text{Im} T_m^a)$ twice.

Thus we finally obtain exactly minus Eq. (4.17). In all of this, one must finally check again that the external mass cuts of the ladder are at least one power of lns down on our leading term.

Since real analyticity implies that B_m in (2.1) is real, it is clear that the correction terms to T_m^a and T_m^b always remain at least one power of lns down on our terms.

The cut shown in Fig. 13 is also rather unfortunate for one's hopes of constructing a linear integral equation for the cut discontinuity from *s*-channel unitarity, since even in the pure multi-Regge region of $(m+1)$ particle phase space it does not factorize.

We would like to stress again that the unitary intermediate states which give the minus sign are exactly those states corresponding to cutting a Reggeon in half. The usual way of drawing Reggeons, as in Fig. 17, is misleading with its

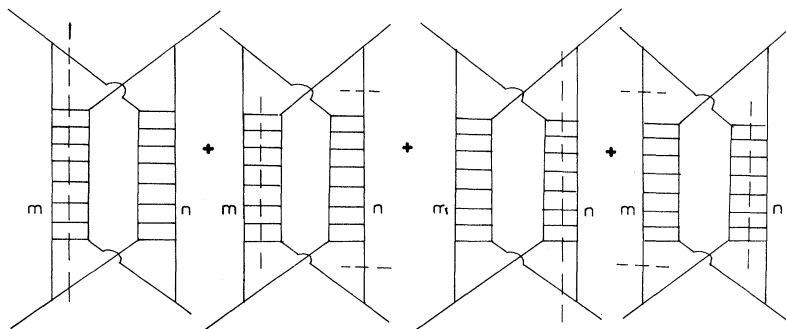


FIG. 15. All the one-Reggeon cuts.

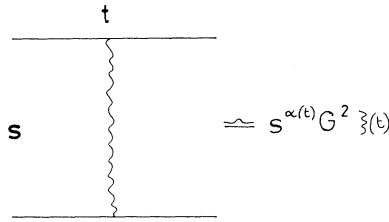


FIG. 17. A Reggeon.

Feynman diagram implication of having no s -channel cuts.

V. THE CUT SIGN

On the basis of the calculation of Sec. IV we wish to state our disagreements with Abarbanel's ansatz.¹² In our view the crucial assumption, which we disagree with, is that if we order our particles by rapidity, whenever we have a large rapidity gap we must have a simple Regge pole exchange as in Fig. 18. These diagrams for production processes *must* be supplemented by diagrams like Fig. 19. When the sum of Fig. 18 and Fig. 19 are introduced into the unitarity equation, we obtain Fig. 20. Term (a) is the Abarbanel ansatz and is clearly positive, however, if (a) also contains the Regge pole output [cf. Ref. 1], then (b) clearly contains two Reggeon cuts of *indeterminate* sign. This is exactly what we have proved in the Mandelstam diagram. Notice Fig. 19 is by no means exhaustive of these possibilities.

Although we agree with almost all of Chew's strictures on perturbation theory models, we would point out that in ϕ^3 theory the trajectory computed from the ladder diagrams $\alpha(t) = -1 + K(t) + O(g^4)$ is believed to be an exact calculation to order g^2 . Thus this trajectory is not renormalized in the approximation by the exchange of itself. These exchanges give rise to a lower trajectory [cf. Ref. 7].

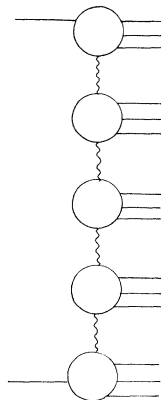


FIG. 18. Abarbanel's ansatz.

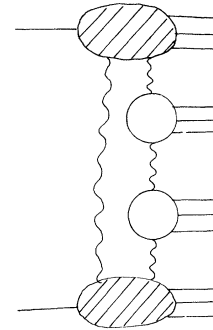


FIG. 19. A correction to Abarbanel's ansatz.

Although one may not like our Feynman diagram-like way of drawing Fig. 19, it is hard to see on what grounds these diagrams or at the very least their s -channel discontinuities can be eliminated from the amplitudes for production processes.

VI. THE INCLUSIVE SUM RULE

DeTar and Weis⁶ show that if we take the inclusive sum rule for energy:

$$(\frac{1}{4}s)^{1/2} \sigma_{tot} = \int \frac{d^3 q_c}{E_c} f(q_c) (E_c), \tag{6.1}$$

and integrate over only the triple-Regge region, then since f is positive

$$(\frac{1}{4}s)^{1/2} \sigma_{tot} \geq \int_{\text{triple Regge}} \frac{d^3 q_c}{E_c} f(q_c) E_c. \tag{6.2}$$

Then in this region, we write f as the diagram in Fig. 21 with Pomeron exchange everywhere we prove dividing by $(\frac{1}{4}s)^{1/2}$

$$\text{const} \geq (\ln \ln s) g_{PPP}(0). \tag{6.3}$$

Hence we find the canonical zero in g_{PPP} . Now the $(\ln \ln s)$ in (6.2) comes from effectively calculating the AFS cut with two Pomerons connected by c . However it is clear that this is canceled by the contribution from diagrams such as Fig. 22. In other words, we are saying there is no cut in the integral of Fig. 21 because there is no fixed pole in the top vertex. Previous examinations of such diagrams¹³ have essentially concentrated on the existence of fixed poles in the central vertex. We could prove this cancellation in our weak coupling model. However the result (6.3) is totally dependent on the Pomeron having $\alpha(0) = 1$. We shall therefore calculate the diagram of Fig. 22 with the Reggeons taken to be Pomerons. We put 2 on-shell and therefore are only computing part of Δ_{M^2} . At the bottom of the diagram, we simply put in a nonzero coupling of the three Pomerons.

Now if we believe that the Regge formalism works for any subenergy $\geq M_0^2$ then the triple-

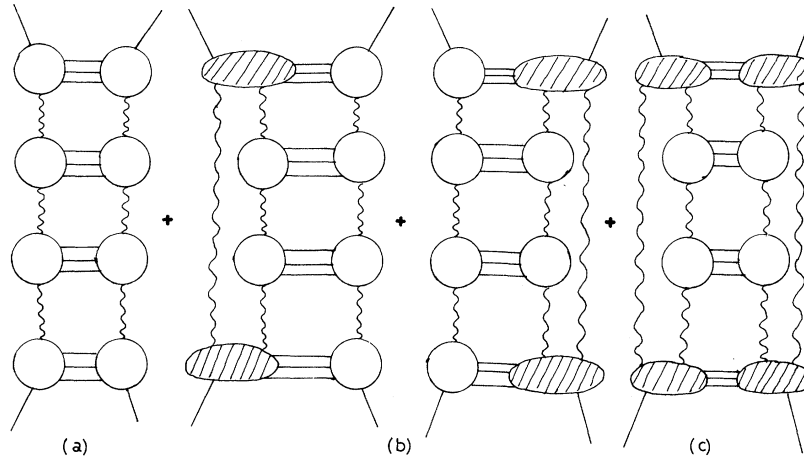


FIG. 20. The unitary contributions.

Regge region corresponds to the α parameter of c lying in the range $1 - M_0^2/s \leq \alpha_1 \leq 1 - m^2/M_0^2$, where m^2 is our particle mass. This ensures that in Fig. 21 the energies appropriate to all three Pomerons $> M_0^2$.

We use the Sudakov variables:

$$\begin{aligned} q_c &= q_1 \\ &= (\alpha_1, \beta_1, \kappa_1), \\ q_2 &= (\alpha_2, \beta_2, \kappa_2). \end{aligned} \tag{6.4}$$

These are both on-shell momenta. Then the missing mass we use is given by

$$\begin{aligned} M^2 &\simeq (q_a + q_b - q_1 - q_2)^2 \\ &\simeq (1 - \alpha_1 - \alpha_2)(1 - \beta_1 - \beta_2)s \geq M_0^2. \end{aligned} \tag{6.5}$$

The energy across the γ Reggeon is then given essentially by $s_\gamma \simeq m^2 s/M^2$, while across the δ Reggeon we have $s_\delta \simeq m^2 s_{2b}/M^2$. It is technically convenient to define $1 - \alpha_1 - \alpha_2 = +\alpha_3$. Thus $M^2 \simeq \alpha_3(1 - \beta_1 - \beta_2)s \geq M_0^2$. Also $s_{2b} \simeq (\alpha_2 s) \geq M_0^2$. Now, as in our AFS integral, the dominant contribution comes from $\alpha_2 \ll \alpha_1$. This is also clearly necessary for us to be looking at the triple-Regge region for particle c .

The two propagators then give

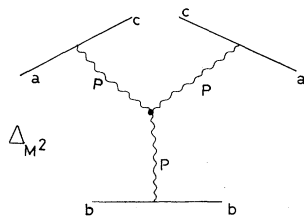


FIG. 21. Triple-Regge contribution.

$$\begin{aligned} (q_\alpha^2 - m^2)^{-1} &\simeq (\beta_2 s)^{-1} \\ &\simeq (\mu_2^2/\alpha_2)^{-1}, \\ (q_\beta^2 - m^2)^{-1} &\simeq -(\mu_\beta^2)^{-1}. \end{aligned} \tag{6.6}$$

Thus, finally we end up with

$$\begin{aligned} J &= -\frac{1}{s} \int d^2\kappa_1 d^2\kappa_2 \int \frac{d\alpha_1}{\alpha_1} \frac{d\alpha_2}{\alpha_2} \frac{1}{(\mu_\beta^2)(\mu_2^2/\alpha_2)} \\ &\quad \times \frac{(s_\gamma/M_\alpha^2)^{\alpha(\kappa_\gamma^2)}}{M_\alpha^2} (s_\delta)^{\alpha(\kappa_\delta^2)} \\ &\quad \times (M^2)^{\alpha(0)} G, \end{aligned} \tag{6.7}$$

where M_α^2 = mass squared in the α line which will be large so we have used the large s and M^2 form valid for the ladder diagrams. G contains all the appropriate coupling functions. Now insert the forms given above for the energies and use $M_\alpha^2 \simeq \mu_2^2/\alpha_2$:

$$\begin{aligned} J &= -\frac{1}{s} \int \frac{d^2\kappa_1}{\mu_2^2} \frac{d^2\kappa_2}{\mu_\beta^2} \int d\alpha_3 \int d\alpha_2 \left(\frac{m^2\alpha_2}{\mu_2^2\alpha_3}\right)^{\alpha(\kappa_\gamma^2)} \\ &\quad \times \left(\frac{m^2\alpha_2}{\alpha_3}\right)^{\alpha(\kappa_\delta^2)} (\alpha_3 s)^{\alpha(0)} \\ &\quad \times G(\kappa_1, \kappa_2), \end{aligned} \tag{6.8}$$

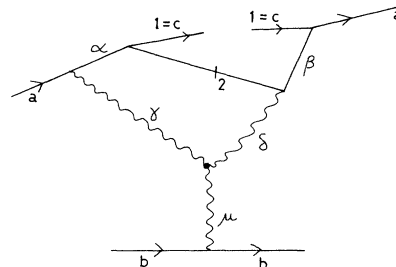


FIG. 22. Another contribution.

where we integrate α_2 from M_0^4/m^2s to μ^2/M_0^2 to stay inside the appropriate Regge regions and α_3 from M_0^2/s to $\alpha_2 m^2/M_0^2$ for the same reason. This means that $1 - \mu^2/M_0^2 \leq \alpha_1 \leq 1 - M_0^4/m^2s$. This is *within* the triple-Regge region which is defined by $1 - \mu^2/M_0^2 \leq \alpha_1 \leq 1 - M_0^2/s$ in our notation. The upper limit is clearly changed by the kinematic necessity of having three large subenergies in Fig. 22. This change does not affect any of the $(\ln \ln s)$ terms as is easily checked.

The kinematics of Fig. 22 also makes sure that $\kappa_\gamma^2 = \kappa_\delta^2$, and we may switch to κ_δ and κ_β as independent integration variables. Now if we have $\alpha(0) = 1$, it is easy to check that the α_3, κ_δ integrals give rise to a term $-(\ln \ln s)A$, where A is a finite integral as $s \rightarrow \infty$. We do not get exact cancellation with the right-hand side of (6.3) except in the weak coupling limit. This is because even with the same c , there are many other Δ_M^2 cuts of Fig. 22 which are equally important in general.

Thus we see that there are other equally large contributions to the sum rule from the same region of phase space as well as that of Fig. 21. Again these are due to the structure of the Reggeon. Because of these additional contributions, we can no longer *obviously* deduce in this way that the triple-Pomeron coupling vanishes. Thus we are forced back to the t -channel proofs given in Ref. 6.

VII. CONCLUSIONS

The results of this paper stress repeatedly that if one attempts to calculate two-Reggeon cuts by using the s -channel unitarity equation, an absolute prerequisite is the knowledge of how the Pomeron itself is reconstructed using s -channel unitarity. This knowledge we do not have at present.

ACKNOWLEDGMENT

One of us (C.T.S.) would like to thank the Science Research Council for a maintenance grant.

APPENDIX

We shall derive the off-shell asymptotic behavior as $s \rightarrow \infty$ as well as one or more masses. The momentum transfer t is at all times kept finite. In order to avoid the normal thresholds in s and M^2 we shall always take the limits where the asymptotic variables tend to $-\infty$.

The Feynman amplitude of Fig. (3a), with Feynman parameters as shown, gives a T matrix given by Ref. 7:

$$T = g^2 \left(\frac{g^2}{16\pi^2} \right)^n \int_0^\infty \prod d\alpha_i d\gamma_j d\delta_k \frac{e^{D/C}}{c^2}, \quad (\text{A1})$$

where D, C are the usual determinants which occur

after performing the symmetric integrations.

Let us first study the limit where $s \rightarrow \infty$ with one M^2 , say, $M_2^2 \rightarrow \infty$. We then write⁷

$$D = fs + gM^2 + d, \quad (\text{A2})$$

where, using the rules of Ref. 7,

$$\begin{aligned} f &= \alpha_1 \alpha_2 \cdots \alpha_{m+1}, \\ g &= \alpha_1 \delta_1 C(m) + \alpha_1 \alpha_2 \delta_2 C(m-1) + \cdots \\ &+ \alpha_1 \alpha_2 \alpha_3 \cdots \alpha_m \delta_m 1, \end{aligned} \quad (\text{A3})$$

where $C(i)$ is the determinant C for the lower i loops. Now let $s = -\sigma$, $M_2^2 = -\xi$ so that we consider $\sigma, \mu^2 \rightarrow +\infty$. Then we define

$$\tilde{A}(\mu, \nu) = \int_0^\infty \sigma^{-\mu-1} \int_0^\infty \xi^{-\nu-1} d\sigma d\xi A(-\sigma, -\xi), \quad (\text{A4})$$

where $A(S, M_2^2) = T(S, M_1^2, M_2^2, M_3^2, M_4^2, t)$ with the nonexplicit variables held fixed. Then by trivial integration,

$$\begin{aligned} \tilde{A}(\mu, \nu) &= \Gamma(-\mu) \Gamma(-\nu) g^2 \left(\frac{g^2}{16\pi^2} \right)^m \\ &\times \int_0^\infty \prod (d\alpha_i d\gamma_j d\delta_k) f^\mu g^\nu \frac{e^{d/c}}{c^{2+\mu+\nu}}. \end{aligned} \quad (\text{A5})$$

We must now enumerate all the singularities in μ, ν of the integral. It is clear by inspection that $c \geq 0$.

The singularities all come from divergences of the integral due to f or g vanishing. By inspection of (A3) we find the following singularities:

- (1) simple pole at $\mu + \nu = -1$ due to $\alpha_1 = 0$;
- (2) m -fold pole at $\mu = -1$ due to $\alpha_2, \alpha_3, \dots, \alpha_{m+1} = 0$ separately;
- (3) simple pole at $\mu + \nu = -2$ due to α_2 and δ_1 simultaneously vanishing;
- (4) simple pole at $\nu = -m - 1$ due to $\delta_1, \delta_2, \dots, \delta_m$ simultaneously vanishing.

There are obviously further poles lying further to the left caused by carrying out further integrations by parts. There are also poles caused by scaling further larger sets of Feynman parameters. These also lie further to the left in a sense that we will clarify during our calculation.

It may be worth stressing at this point that some scalings which apparently give different types of singularity must be treated with caution. Thus, apparently, if we scale α_1, α_2 by ρ , we obtain the integral

$$\int_0^\infty \rho d\rho \delta(\alpha_1 + \alpha_2 - 1) (\alpha_1 \alpha_2)^\mu \alpha_1^\nu \frac{e^{d/c}}{c^{2+\mu+\nu}} d\alpha_1 d\alpha_2 \rho^{2\mu+\nu}, \quad (\text{A6})$$

which apparently has a singularity at $2\mu+\nu=-2$ due to the ρ integration. However the two integrals over $\alpha_1 \sim 0$ and $\alpha_2 \sim 0$, respectively, give rise to a factor

$$\left\{ \frac{1}{\mu+\nu+1} + \frac{1}{\mu+1} \right\},$$

which cancels the $2\mu+\nu=-2$ singularity.

The coefficient of the multiple poles given by singularities (1) and (2) is equal to the usual Regge-limit coefficient since we have integrated by parts the same variables as in the Regge limit:

$$\tilde{A}(\mu, \nu) \simeq \frac{\Gamma(-\mu)\Gamma(-\nu)g^2}{(\mu+\nu+1)(\mu+1)^m} [K(t)]^m. \quad (\text{A7})$$

We now invert (A7) using the formula

$$A(s, M^2) = \int_{-i\infty}^{i\infty} (-s)^{+\mu} (-M^2)^{+\nu} \frac{\tilde{A}(\mu, \nu)}{(2\pi i)^2} d\mu d\nu. \quad (\text{A8})$$

Since we are interested in $S \gg M^2$, we first of all carry out the ν integration. Using (A7) we find

$$A(s, M^2) \simeq \int_{-i\infty}^{i\infty} \frac{d\mu}{(2\pi i)} (-s)^\mu \frac{g^2 K^m}{(\mu+1)^m} \times \Gamma(-\mu)\Gamma(\mu+1)(-M^2)^{-\mu-1}. \quad (\text{A9})$$

Since $|s/M^2| \rightarrow \infty$, we see that the right-most pole

in μ gives the dominant contribution. Notice that $\Gamma(\mu+1)$ also has a pole at $\mu=-1$, so that we end up with an $(m+1)$ -fold pole at $\mu=-1$. This is caused, in general, in (A5) by the ν contour being pinched between the $\nu=0$ pole of the Γ function lying to the right of the ν contour and the $\mu+\nu=-1$ pole lying to the left at $\mu=-1$.

Moving the μ contour to the left now gives

$$A(s, M^2) \simeq \frac{-g^2 K^m [\ln(-s/-M^2)]^m}{m! s}. \quad (\text{A10})$$

This is the result assumed in (2.5). We claim that none of the extra singularities coming from larger sets of scalings interferes with these results. We leave this as a straightforward but rather tedious check for the reader.

The results of Eqs. (2.6) and (2.7) are obtained in the same way by defining triple Mellin transforms with respect to s and the two masses. The singularities are then essentially identical to those found above, and the required results (2.6) and (2.7) are easily verified.

The only tricky point is to always make sure that the Mellin inversion is performed on the *smallest* variables first.

If $s/M^2 \rightarrow 0$, then in (A8) the integrations must be performed in the opposite order. This leads to quite different results which we hope to examine later.

¹H. D. I. Abarbanel, Phys. Rev. D 6, 2788 (1972); G. F. Chew, *ibid.* 7, 934 (1973).

²A. R. White, Nucl. Phys. B 50, 130 (1972).

³D. Amati, S. Fubini, and A. Stanghellini, Nuovo Cimento 26, 896 (1962).

⁴L. Caneschi, Phys. Rev. Lett. 23, 254 (1969); J. W. Dash, J. R. Fulco, and A. Pignotti, Phys. Rev. D 1, 3164 (1970).

⁵H. F. Rothe, Phys. Rev. 159, 1471 (1967); V. N. Gribov, Zh. Eksp. Teor. Fiz. 53, 654 (1967) [Sov. Phys.-JETP 26, 414 (1968)].

⁶C. E. DeTar and J. H. Weis, Phys. Rev. D 4, 3141 (1971); C. E. Jones, F. E. Low, S. H. Tye, G. Veneziano, and J. E. Young, *ibid.* 6, 1033 (1972); H. D. I. Abarbanel and M. B. Green, Phys. Lett. 38B, 90 (1972); P. Goddard and A. R. White, *ibid.* 38B, 93 (1972); J. B. Bronzan, Phys. Rev. D 6, 1130 (1972).

⁷R. J. Eden, P. V. Landshoff, D. I. Olive, and J. C. Polkinghorne, *The Analytic S-Matrix* (Cambridge Univ. Press, Cambridge, England, 1966).

⁸G. Altarelli and H. R. Rubinstein, Phys. Rev. 187, 2111

(1969).

⁹J. C. Polkinghorne, Phys. Lett. 4, 24 (1963); S. Mandelstam, Nuovo Cimento 30, 1127 (1963); 30, 1148 (1963); P. Nicoletopoulos and M.A.L. Prevost, *ibid.* 5A, 357 (1971).

¹⁰V. Sudakov, Zh. Eksp. Teor. Fiz. 30, 87 (1956) [Sov. Phys.-JETP 3, 65 (1956)]; I. G. Halliday and L. M. Saunders, Nuovo Cimento 60A, 115 (1969).

¹¹G. M. Cicuta and R. L. Sugar, Phys. Rev. D 3, 970 (1971). We would warn the careful reader that this disagrees with the calculation in Ref. 7.

¹²We also disagree with one of Abarbanel's technical statements. A Reggeon-Reggeon scattering amplitude has as well as normal thresholds a cut in s starting at the origin. Thus Abarbanel's unitary integral is not the total right-hand discontinuity of the Reggeon-Reggeon amplitude. Cf. I. G. Halliday, Nucl. Phys. B 21, 445 (1970).

¹³S.-J. Chang, D. Gordon, F. E. Low, and S. B. Treiman, Phys. Rev. D 4, 3055 (1971).